BIOSYSTEMS ENGINEERING 186 (2019) 349–355

Available online at www.sciencedirect.com

ScienceDirect

journal homepage: www.elsevier.com/locate/issn/15375110

Research Paper

Estimating bond damping and bond Young's modulus for a flexible wheat straw discrete element method model

Matthew Schramm [a], Mehari Z. Tekeste [a,*], Carol Plouffe [b], Donald Harby [b]

[a] Iowa State University, United States
[b] Deere & Company, United States

ARTICLE INFO

Article history:
Received 17 September 2018
Received in revised form
4 August 2019
Accepted 7 August 2019
Published online 11 September 2019

Keywords:
DEM Calibration
Flexible Fibre
LIGGGHTS
Discrete Element Method

A method to calculate the local damping coefficient and the bond Young's modulus of a flexible fibre for use in the discrete element method (DEM) was proposed and validated. Segments of harvested wheat straw were clamped on one end while the other end was deflected a set distance, released, and allowed to vibrate freely. This cantilever beam motion was captured by a high-speed camera (960 fps). The red-band of the images were isolated and used to calculate the x-section height (mm) along the stem in time. This data was then fit to a non-linear function, which conforms to beam theory. The global bond damping coefficient, as a function of x-section height, was then calculated and found to be in the range of −0.5 to −0.2. The cantilever beam experiment was then repeated in the DEM software LIGGGHTS, where the wheat straw was modelled as a single line of spheres connected by stiff-flexible bonds. A design of experiment (DOE) was ran varying bond Young's modulus and local bond damping, to determine the linear relationships with the global bond damping coefficient and the frequency of oscillation of the DEM particle respectively. With the proposed method the DEM local bond damping coefficient and the DEM bond Young's modulus were calibrated with relative errors of 0.9% and 1.8% respectively to laboratory estimated values. Utilising the linear relationships found from the DEM simulations, the bond Young's modulus was found to be in the range of 0.42–4.84 GPa.

1. Introduction

With the continued improvements in computational speed, researchers have begun to utilise simulation-based design for complex engineering problems. The discrete element method (DEM) has recently been shown to be a powerful tool in simulating discrete flows of granular and fibrous systems. One of the many challenges to overcome in DEM, is the determination of the micro-interaction parameters that determine particle–particle and particle–geometry interactions. This is due to how both particles and interactions of particles are numerically approximated in the simulation. DEM codes approximate a material by a simple numerical geometric shape, mostly a sphere (e.g. soybean), or clumped/glued spheres to approximate irregular shaped particles (e.g. corn).

* Corresponding author.
E-mail address: mtekeste@iastate.edu (M.Z. Tekeste).
https://doi.org/10.1016/j.biosystemseng.2019.08.003

Using these to approximate a given material, it is common to use laboratory acquired material properties as a starting point in calibrating a DEM particle model. Potyondy and Cundall (2004) provided a way to approximate rock as a dense packing of non-uniformly sized spheres bonded together. This bond model has since been extended to approximate fibrous materials (e.g. wheat straw) but provided no means of capturing the damping behaviour observed in fibrous material. Using Potyondy's and Cundall's model as a stepping stone, multiple bond models began to be implemented by the DEM community. These models ranged from cohesion models (Wittel, Kun, & Herrmann, 2006), spring and damper models (Park & Kang, 2009; Lenaerts et al., 2014), to bond elastic wave models (Guo, Curtis, Wassgren, Ketterhagen, & Hancock, 2013a). With the additions of these bond models, a method to determine the damping coefficient has yet to be brought forward. In most of the above methods, the authors either choose an arbitrary value for the local bond damping coefficient or tuned the coefficient until the simulation of the material showed the qualitative behaviour (Lenaerts et al., 2014).

Park and Kang (2009) used a relationship including the spring coefficient and the coefficient of restitution to calculate the normal damping while the coefficient of friction is used for tangential energy dissipation. While the coefficient of restitution and friction can be measured, it is often difficult to have a flexible fibre behave in such a matter to collect reliable data. There do exist multiple sources where material properties for fibres can be experimentally estimated (Galedar et al., 2008; Adapa, Tabil, & Schoenau, 2010; Afzalinia & Roberge, 2007).

The objective of this study is (1) determine global damping of wheat straw based on cantilever beam theory, (2) develop a relationship between the global damping coefficient (as measured by the entire fibre) and the local damping coefficient (as measured between two spheres) for DEM simulations, and (3) develop a relationship between the period of oscillation and the bond stiffness coefficient. By providing calibration techniques, manufactures can run more accurate simulations to reduce the time and money associated with bringing a product to market.

2. Methods and materials

2.1. Data acquisition

Wheat straw were harvested from the Iowa State University Research Farm located in Boone Iowa, USA. Individual wheat straw stems were separated from the shell and cut such that there were no samples of the wheat straw containing a node (each wheat straw was a hollow cylinder). Thirty samples of the hollow cylindrical processed wheat straw were randomly selected and cut such that a mean length of 156 mm was observed above the wire clamp. An aluminium pin (2.25 mm diameter) was placed inside the hollow wheat straw at one fixed end such that a wire clamp did not crimp the straw (Fig. 1). The wheat straw with fixed end was put on a flat plane and the other end was deflected horizontally to a mean deflection of 25 mm by hand by using the tip of a finger on the

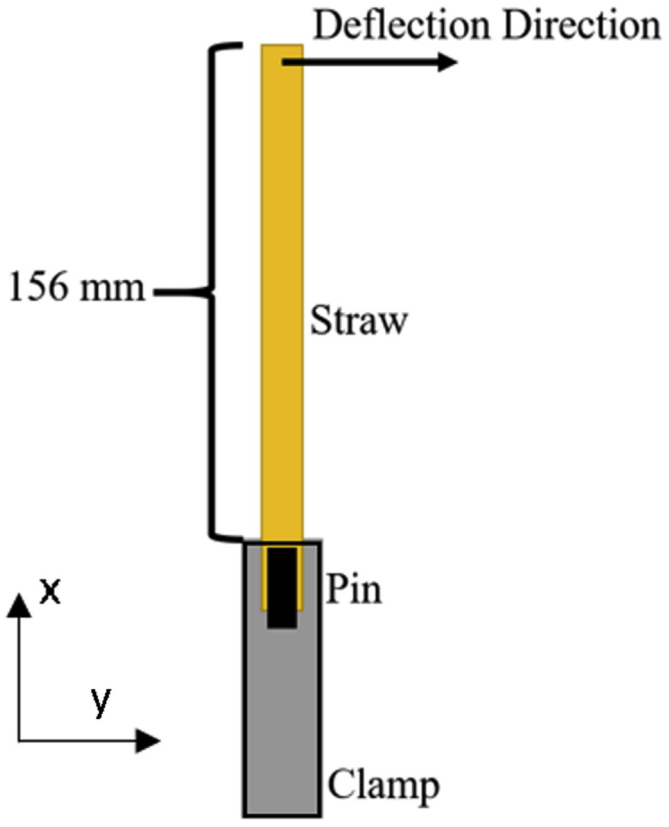

Fig. 1 – Schematic of laboratory test. A hollow wheat straw has an aluminium pin placed inside of it to stop crimping caused by the wire holder clamp.

top of the straw. The straw was then released by hand immediately allowing the straw to oscillate. This oscillation was recorded by a high-speed camera (Sony NEX-FS700) at 960 frames per second (fps).

2.2. Data analysis

MATLAB (version R2017b, www.mathworks.com) was used to analyse the high-speed video data. The video frames were split into the red, blue, and green spectrums of light. The red band was then used to create logical video frames of the wheat straw stems during the oscillation (Fig. 2a) as the red band provided a clearer image for analysis. The row median of the logical image was then used as the stem's central location and was used to fit a quadratic linear model of the wheat stem position in the x-direction (Fig. 2b). The median was used to minimise artefacts of the logical image. The linear model was used as a preliminary step to calculate the trajectory of the wheat stem as a function of stem height (x) during damping.

The displacement of the stem was then tracked with time per stem height (Fig. 3a) and the dataset was then trimmed to just before stem release to when the oscillation of the stem ceased (Fig. 3b). The time axis was normalised by setting the time to zero at the moment the stem was released and dividing the time by the period of the observed oscillation, and the deflection was normalised by the maximum deflection (Fig. 3c). This was done as a preliminary step to fit the non-linear function (Eq. (1)).

$$y(t) = b_0 e^{b_1 t} \cos(2\pi b_2 t) \quad (1)$$

Where

- $y(t)$ is the deflection of the stem at time equal to t at a specific height along the wheat stem
- b_0 is the initial deflection of the wheat stem
- b_1 is the global damping coefficient
- b_2 is the oscillation frequency

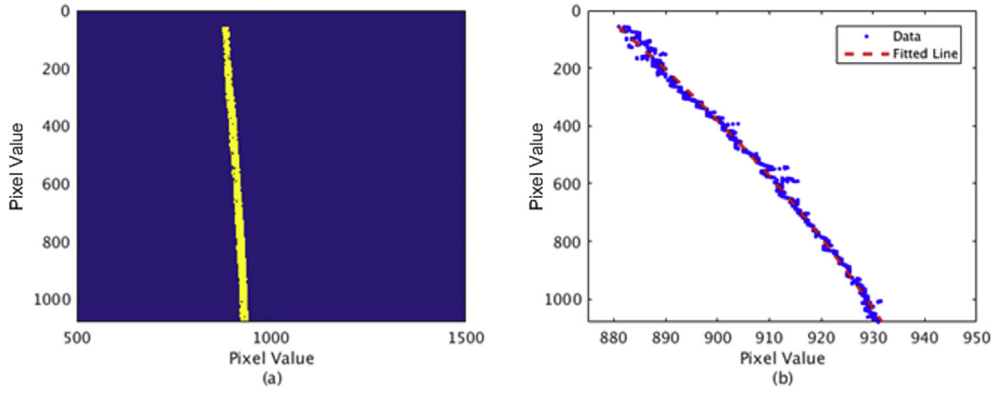

Fig. 2 – Logical image of wheat straw in red band (a). Quadratic fit of the median pixel location as a function of height of the logical image of the wheat straw (b).

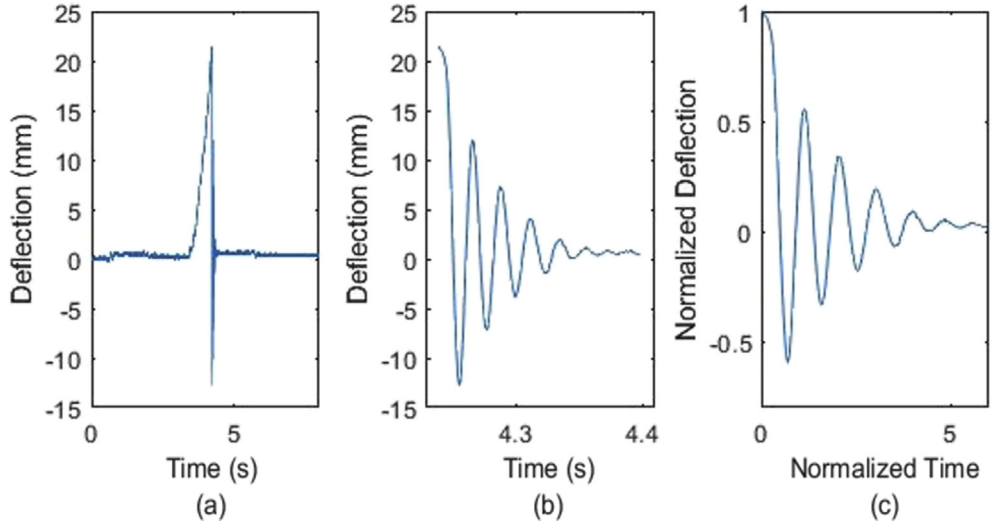

Fig. 3 – Displacement (measured) of wheat straw at specific height of stem (a). Dataset reduced to just before release and stem has reached equilibrium (b). Dataset normalised in both time and deflection. Time is normalised by observed period of oscillation and displacement is divided by max deflection (c).

Eq. (1) was used as it is a proposed solution to the differential equation that describes damped harmonic motion (Eq. (2)).

$$\frac{d^2y}{dt^2}+2\zeta\omega\frac{dy}{dt}+\omega^2y=0 \tag{2}$$

Where

- y is the deflection distance
- ω is the oscillation frequency
- ζ is the damping ratio

Although ω and b_2 both describe the frequency in which the fibre oscillates, b_2 can be measured directly while ω can only be calculated knowing the bond stiffness value. Ideally, the relationship $\omega=\frac{b_2}{2\pi}$ should hold but cannot be guaranteed.

2.3. DEM simulation of wheat straw cantilever test

A discrete element method (DEM) simulation design of experiments (DOE) was ran to investigate the DEM parameters sensitive to the cantilever test and to compare simulation to the observed wheat straw lab experiments. The open-source DEM software LIGGGHTS (version 3.7) (Kloss, Goniva, hager, Amberger, & Pirker, 2012) was chosen to perform the DEM simulations. A modified version of LIGGGHTS developed by Richter (2015) that included the bond equations was further developed to include the bond damping equations (Eqs (3)–(10)) (Guo et al., 2013a). For the DEM simulation, a mega-particle comprised of 56 spheres (2.83 mm diameter) was used to represent a piece of wheat straw (Fig. 4). This fully modified copy of LIGGGHTS gave comparable results to Guo, Wassgren, Hancock, Ketterhagen, and Curtis (2013b). The diameter of 2.83 mm was chosen due to the results of an earlier straw characterisation sampling.

One end of the mega-particle was held fixed by a single sphere while the other end was deflected to 15 mm, once the mega-particle came to rest, the deflected end was then allowed to vibrate freely for 0.01 s. The discrepancy between the simulation and laboratory deflection distances was to allow the simulations to finish in a reasonable amount of time. This process was repeated for eight different values of the bond damping coefficients and ten different values of bond Young's modulus. The values, 25, 50, 75, 100, 125, 150, 175, and 200 were used in Eqs. (3)–(10) as the DEM local bond damping coefficient (β_{damp}), and the values 1 GPa, 2 GPa, 3 GPa, 4 GPa, 5 GPa, 6 GPa, 7 GPa, 8 GPa, 9 GPa, and 10 GPa were used for the bond Young's modulus, to calculate the DEM bond forces (F_n^b and F_t^b) and bond moments (M_n^b and M_t^b) for both normal and tangential components (Eqs (3)–(10)). Utilising these ranges of values, a full factorial DOE was done for a total of 80 runs. Eq. (11) is used to calculate K_n and K_t.

$$\delta F'^{b}_{n,i}=K_tA_b\upsilon_n\Delta t \tag{3}$$

$$\delta F'^{b}_{t,i}=K_tA_b\upsilon_t\Delta t \tag{4}$$

$$\delta M'^{b}_{n,i}=K_tI_p\omega_n\Delta t \tag{5}$$

$$\delta M'^{b}_{t,i}=K_nI\omega_t\Delta t \tag{6}$$

$$F_n^b=\sum\nolimits_{\forall i}\delta F'^{b}_{n,i}+2\beta_{damp}\sqrt{M_eK_n}\upsilon_n \tag{7}$$

$$F_t^b=\sum\nolimits_{\forall i}\delta F'^{b}_{t,i}+2\beta_{damp}\sqrt{M_eK_t}\upsilon_t \tag{8}$$

$$M_n^b=\sum\nolimits_{\forall i}\delta M'^{b}_{n,i}+2\beta_{damp}\sqrt{J_sK_tI_p}\omega_n \tag{9}$$

$$M_t^b=\sum\nolimits_{\forall i}\delta M'^{b}_{t,i}+2\beta_{damp}\sqrt{J_sK_nI}\omega_t \tag{10}$$

$$K_n=\frac{Y}{l_b},\ K_t=\frac{K_n}{2(1-\nu)} \tag{11}$$

where (Guo et al., 2013a)

- F_n^b, F_t^b are the normal and tangential bond forces, respectively
- M_n^b, M_t^b are the normal and tangential bond moments, respectively
- $\delta\acute{F}^b_{n,i}$, $\delta F'^{b}_{t,i}$ are the normal and tangential ith incremental bond forces caused by the linear spring, respectively
- $\delta\acute{M}^b_{n,i}$, $\delta\acute{M}^b_{t,i}$ are the normal and tangential ith incremental bond moments caused by the linear spring, respectively
- K_n and K_t are the normal and tangential bond stiffness constants, respectively
- A_b is the bond cross sectional area
- Δt is the time step
- β_{damp} is the local bond damping coefficient
- M_e and J_s are the mass and moment of inertial of the individual particles, respectively
- υ_n and υ_t are the normal and tangential relative velocities between the two particles, respectively
- w_n and w_t are the normal and tangential relative angular velocities between the two particles, respectively
- I and I_p are the second area moment and polar area moments of inertia, respectively
- Y is the bond Young's modulus
- ν is the Poison's ratio
- l_b is the equilibrium bond length

It should be noted that there is a discrepancy between the above equations and what is found in Guo et al. (2013a). The authors chose to use a factor of 2 rather than a factor of $\sqrt{2}$ as the constant 2 more closely resembles what is seen in Eq. (2).

This bond model assumes that two particles are bonded together via a spring and damper system. Guo et al. (2013b) has shown that the non-damped bonds reproduce beam behaviours as described by the Euler-Bernoulli beam equations (Guo et al., 2013b). A shortcoming to the bond equations in the

Fig. 4 – Mega-Particle representation of a wheat straw stem for DEM simulations consisting of 56 spheres.

handling of damping. If the local bond damping coefficient β_{bond} is large, the bond equations become stiff and require very short time steps to be stable.

After the DEM simulations, the global damping coefficient (b_1) and oscillation frequency (b_2) was estimated using the same process as used for the laboratory experiment of wheat straw mentioned above (Eq. (1)). Table 1 shows the DEM material parameters that were used for the simulations. Bond diameter and bond length were selected to be the stem's diameter. The particle density was found from a random sample of stems utilizing the average mass and average volume (assuming the stem was a solid cylinder) of this sample. Density was then calculated taking the average mass and dividing it by the average volume. Poisson's ratio and contact Young's modulus were selected from literature (Hamman et al., 2005; O'Dogherty, Huber, Dyson, & Marshall, 1995; Stasiak, 2003).

3. Results and discussion

3.1. Laboratory results

The mean wheat straw length was measured to be 156 mm (standard deviation of 4.5 mm), a mean diameter of 2.57 mm (standard deviation of 0.45 mm) and a mean thickness of 0.34 mm (standard deviation of 0.08 mm). The moisture content of the wheat was measured to be 5.8% dry basis. The maximum deflection of each stem utilising the captured video was found to have a mean of 23.6 mm (standard deviation of 5.3 mm). The global damping coefficient (b_1) and frequency of oscillation (b_2) as a function of x-section stem height was then calculated for 29 samples. One test was removed due to the stem breaking during the deflection process. Figure 5 shows the results of the global bond damping coefficient and the observed frequency of oscillation. For the wheat stems that were tested, the global damping coefficient normalised by the max deflection of a given stem was found to have a mean value of −0.46 (standard deviation of 0.17) and the mean frequency was found to be 64.6 Hz (standard deviation of 21.2 Hz).

Figure 6 displays the normalised global bond damping coefficient as a function x-section stem height and as a function of the stem's aspect ratio. The aspect ratio was calculated by dividing the stem length by the stem diameter. As can be seen in Fig. 6a, there appears to be no clearly defined relationship between the global damping coefficients (b_1) and the stem dimensional properties. However, in Fig. 6a, banding was observed in the form of a linear dependency if looking at an individual stem, as a function of x-section stem height. Viewing the data circled (from stem #22), the base of the stem has a damping ratio of −0.2 and linearly decreases to the tip of the stem. Aspect ratio of a stem's length to its diameter showed no correlation to the normalised global damping coefficient (Fig. 6b).

Table 1 – DEM parameters for wheat stem DEM simulation.

Parameters	Values	Units
Particle diameter	2.83	mm
Bond diameter	2.83	mm
Bond length	2.83	mm
Particle density	125	kg m^{-3}
Particle Contact Young's Modulus	4.4	GPa
Particle Poison's Ratio	0.3	
Time Step (Δt)	1.0e-10	s

3.2. DEM simulation

Figure 7a illustrates the effect of the bond Young's modulus (Y) on the period of oscillation of the wheat stem while Fig. 7b illustrates the effect of the local bond damping coefficient (β_{local}) on the global damping coefficient (b_1) of the wheat stem. Both figures are using selective values as to not over saturate the figures. For Fig. 7a a value of 150 was held constant for the local bond damping coefficient and the bond Young's modulus was set to 1, 5, and 10 GPa. In Fig. 7a it was observed that as the bond Young's modulus increased, so did the frequency of oscillation while appearing to have no effect on the global damping of the wheat stem per oscillation as the heights appeared to be similar for each plot per full cycle. This was later confirmed during model selection. For Fig. 7b a value of 10 GPa was held constant for the bond Young's modulus while the local bond damping coefficient was set to 25, 100,

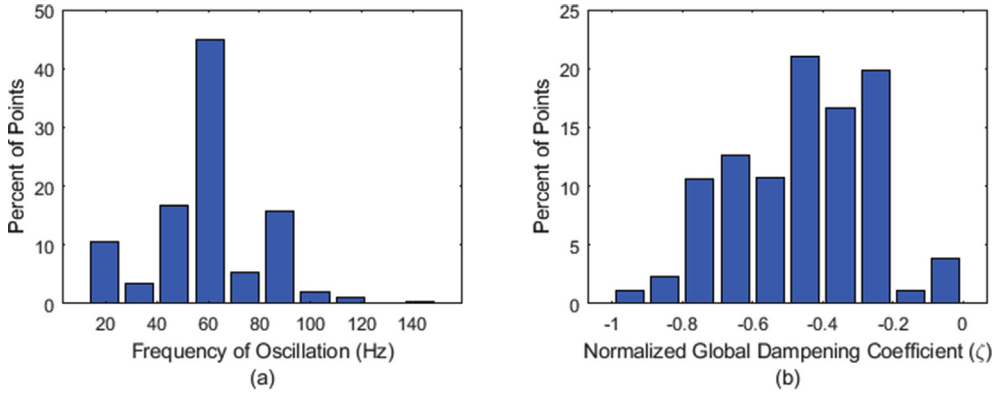

Fig. 5 – Histogram of observed frequencies of oscillations of wheat stems (a). Histogram of observed global bond damping coefficient of wheat straw stems normalised by the maximum deflection (b).

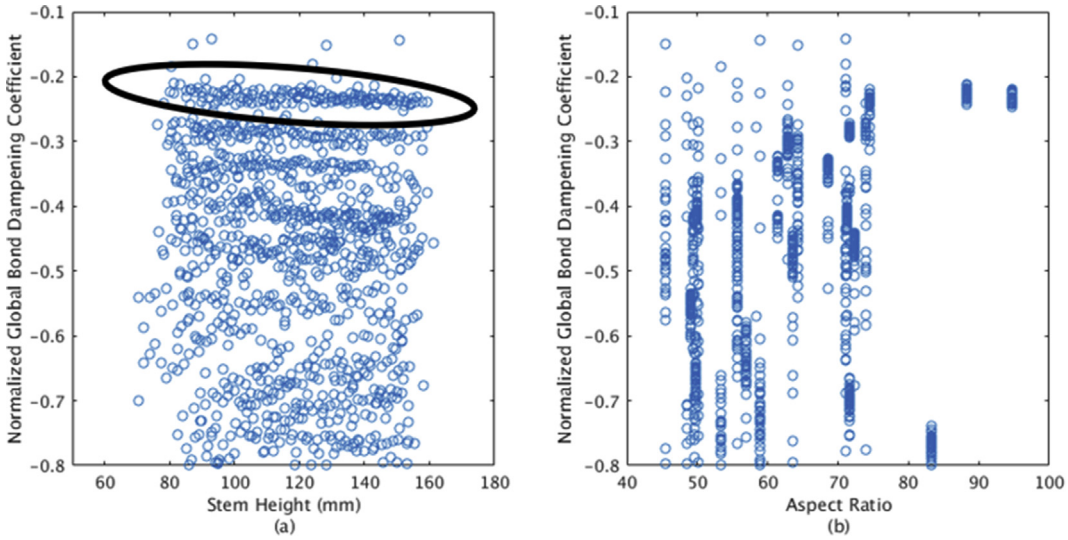

Fig. 6 – Graph showing interaction of stem height on the global damping coefficient (b_1). Banding is seen from stem #22 (circled)(a). Graph showing the effect of aspect ratio on the global damping coefficient (b).

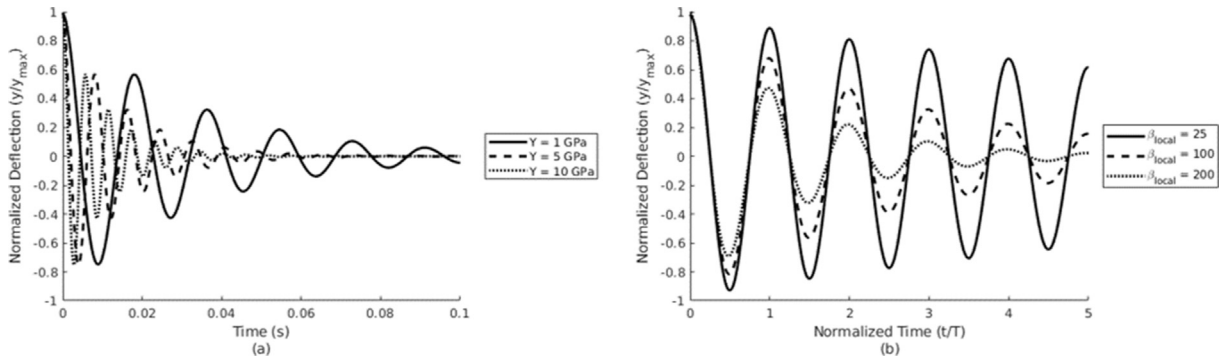

Fig. 7 – Plot showing the effect of selective bond Young's modulus on the frequency of the oscillation of the fibre while holding the local bond damping coefficient at a constant value of 150 (a). Plot showing the effect of selective local bond damping coefficient on the rate of observed global damping of the flexible fibre while holding the bond Young's modulus at a constant value of 10 GPa (b).

and 200. From Fig. 7b, it was observed that as the local bond damping coefficient was increased, so did the global bond damping coefficient of the simulated wheat stem.

Figure 8 shows the histograms of the percent error of two linear models that predict the DEM parameters of bond Young's modulus (Fig. 8a) and the local bond damping

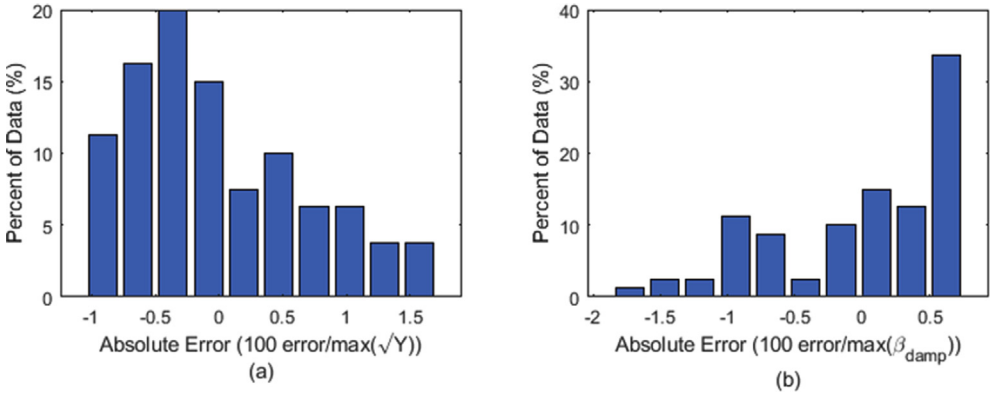

Fig. 8 – Absolute Error histogram of the residuals in the linear models for the prediction of the bond Young's modulus (a) and the local bond damping coefficient (b).

coefficient (Fig. 8b). Where the percent error was calculated by taking the difference of the laboratory measured value and the model predicted value and dividing the difference by the maximum observed laboratory value. The linear model for the bond Young's modulus, in Pascals, can be seen in Eq. (12) using normalised displacement and not normalised time, and the local bond damping coefficient linear model can be seen in Eq. (13) using both normalised displacement and normalised time. Models were developed by first fitting the full interaction linear model and then linear terms were removed utilizing a nested model selection F-test where the reduced model was rejected if the p-value was less than 0.05.

$$\sqrt{Y} = 574.3b_2 + 91.4 \tag{12}$$

$$\beta_{damp} = -261.4b_1 + 2.5 \tag{13}$$

Where b_1 and b_2 are the coefficients found using Eq. (1) in the laboratory. Both models (Eqs. (12) and (13)) yielded an adjusted R^2 greater than 0.999. Utilising Eq. (12), it was found that 90% of stems maintained a Young's modulus between 0.42 and 4.84 GPa. Using Eqs. (12) and (13), one can now estimate what the DEM simulation parameters. As an example, given a stem yielded a normalised global damping coefficient (b_1) of 0.64, and a frequency of oscillation (b_2) of 113.1 Hz, the estimated DEM simulation parameters will be 4.23 GPa and 164.80 for the bond Young's modulus and local bond damping coefficient, respectively. Running a DEM simulation of the cantilever beam using the bond Young's modulus value of 4.23 GPa, local bond damping coefficient of 164.80 and the remaining DEM parameters in Table 1, the simulated wheat stem yielded an error of the frequency of oscillation (b_2) measurements of 1.8% between the simulation and laboratory, and an error 0.9% between the simulated and lab measured normalised global bond damping coefficients (b_1).

4. Conclusions

The bond damping model as described by Guo et al. (2013a) was implemented in the DEM software LIGGGHTS. The bond DEM model was used to simulate a cantilever beam test of a wheat straw. The simulation was able to reproduce the exponential decay of the global damping (b_1) that was observed in laboratory experiment. Furthermore, the simulation was able to reproduce the global bond damping coefficient that matches the observed mean local bond damping coefficients within 0.9% relative error. This was mirrored for the bond Young's modulus with a relative error of 1.8%. With the measurement and calibration of bond damping proposed in this study, future works will be conducted to investigate how such measurements and calibration techniques can be integrated into bulk DEM simulations of flexible fibres and investigate the time step sensitivity and how it is affected by the local bond damping coefficient.

Acknowledgement

The authors would like to thank John Deere for providing financial support for this project and allowing the release of the results found in this paper. Any queries relating to the raw data should be directed to the authors.

REFERENCES

Adapa, P., Tabil, L., & Schoenau, G. (2010). Physical and frictional properties of non-treated and steam exploded barley, canola, oat and wheat straw grinds. *Powder Technology, 201*(3), 230–241.

Afzalinia, S., & Roberge, M. (2007). Physical and mechanical properties of selected forage materials. *Canadian Biosystems Engineering, 49*, 2.

Galedar, M. N., Jafari, A., Mohtasebi, S. S., Tabatabaeefar, A., Sharifi, A., O'Dogherty, M. J., et al. (2008). Effects of moisture content and level in the crop on the engineering properties of alfalfa stems. *Biosystems Engineering, 101*(2), 199–208.

Guo, Y., Curtis, J., Wassgren, C., Ketterhagen, W., & Hancock, B. (2013a). Granular shear flows of flexible rod-like particles. *AIP Conference Proceedings, 1542*, 491. https://doi.org/10.1063/1.4811975.

Guo, Y., Wassgren, C., Hancock, B., Ketterhagen, W., & Curtis, J. (2013b). Validation and time step determination of discrete element modeling of flexible fibers. *Powder Technology, 249*, 386–395.

Hamman, K. D., Williamson, R. L., Steffler, E. D., Wright, C. T., Hess, J. R., & Pyrfogle, P. A. (2005). Structural analysis of wheat stems. *Applied Biochemistry and Biotechnology, 121–124*, 71–80.

Kloss, C., Goniva, C., hager, A., Amberger, S., & Pirker, S. (2012). Models, algorithms and validation of opensource DEM and CFD-DEM. *Progress in Computational Fluid Dynamics An International Journal, 12*(2/3), 140–152. https://doi.org/10.1504/PCFD.2012.047457.

Lenaerts, B., Aertsen, T., Tijskens, E., De Ketelaere, B., Ramon, H., De Baerdemaeker, J., et al. (2014). Simulation of grain–straw separation by Discrete Element Modeling with bendable straw particles. *Computers and Electronics in Agriculture, 101*, 24–33.

O'Dogherty, M. J., Huber, J. A., Dyson, J., & Marshall, C. J. (1995). A study of the physical and mechanical properties of wheat straw. *Journal of Aricultural Engineering Research, 62*, 133–142.

Park, J., & Kang, N. (2009). Applications of fiber models based on discrete element method to string vibration. *Journal of Mechanical Science and Technology, 23*(2), 372–380.

Potyondy, D., & Cundall, P. (2004). A bonded-particle model for rock. *International Journal of Rock Mechanics and Mining Sciences, 41*, 1326–1364.

Richter, C. (2015). *Liggghts-with-bonds*. GitHub Repository. https://github.com/richti83/LIGGGHTS-WITH-BONDS.

Stasiak, M. (2003). Determination of elastic parameters of grain with oedometric and acoustic methods. *Research in Agricultural Engineering, 49*(2), 56–60.

Wittel, F. K., Kun, F., & Herrmann, H. J. (2006). Particle models: Simulation of damage and fracture in composites using a discrete element approach. In G. Busse, B. Kröplin, & F. K. Wittel (Eds.), *Damage and its evolution in fiber-composite materials* (p. 2006). Stuttgart: ISD Verlag, ISBN 3-930683-90-3.